Diverse Regulators of Human Ribosome Biogenesis Discovered by Changes in Nucleolar Number

Katherine I. Farley-Barnes[1,6], **Kathleen L. McCann**[2,3,6], **Lisa M. Ogawa**[1], **Janie Merkel**[4], **Yulia V. Surovtseva**[4], and **Susan J. Baserga**[1,2,5,7,*]

[1]Department of Molecular Biophysics and Biochemistry, Yale University School of Medicine, New Haven, CT 06520, USA

[2]Department of Genetics, Yale University School of Medicine, New Haven, CT 06520, USA

[3]Epigenetics and Stem Cell Biology Laboratory, National Institute of Environmental Health Sciences, NIH, PO Box 12233 MD F3-05, Research Triangle Park, NC 27709, USA

[4]Yale Center for Molecular Discovery, Yale University, 600 West Campus Drive, West Haven, CT 06516, USA

[5]Department of Therapeutic Radiology, Yale University School of Medicine, New Haven, CT 06520, USA

SUMMARY

Ribosome biogenesis is a highly regulated, essential cellular process. Although studies in yeast have established some of the biological principles of ribosome biogenesis, many of the intricacies of its regulation in higher eukaryotes remain unknown. To understand how ribosome biogenesis is globally integrated in human cells, we conducted a genome-wide siRNA screen for regulators of nucleolar number. We found 139 proteins whose depletion changed the number of nucleoli per nucleus from 2–3 to only 1 in human MCF10A cells. Follow-up analyses on 20 hits found many (90%) to be essential for the nucleolar functions of rDNA transcription (7), pre-ribosomal RNA (pre-rRNA) processing (16), and/or global protein synthesis (14). This genome-wide analysis exploits the relationship between nucleolar number and function to discover diverse cellular pathways that regulate the making of ribosomes and paves the way for further exploration of the links between ribosome biogenesis and human disease.

Graphical abstract

*Correspondence: susan.baserga@yale.edu.
[6]These authors contributed equally
[7]Lead Contact

SUPPLEMENTAL INFORMATION
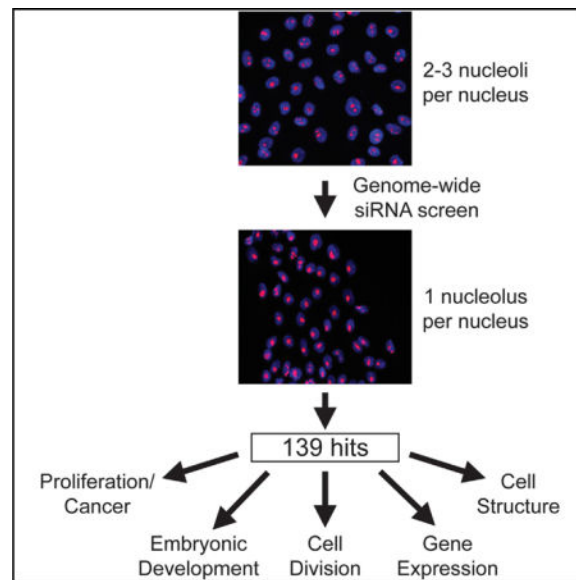Supplemental Information includes Supplemental Experimental Procedures, five figures, and four tables and can be found with this article online at https://doi.org/10.1016/j.celrep.2018.01.056.

DECLARATION OF INTERESTS
The authors declare no competing interests.

INTRODUCTION

Ribosome biogenesis is a highly regulated cellular process essential for growth and development. In humans, production of ribosomes begins in the cell nucleolus with the transcription of a 47S precursor rRNA (pre-rRNA) by RNA polymerase I (RNAPI). This 47S pre-rRNA is transcribed from the 5 acrocentric chromosomes in humans (13, 14, 15, 21, and 22) that bear the repeated rDNA sequences. The 47S pre-rRNA is chemically modified and processed before assembly with the 5S rRNA into the mature ribosomes that are essential for protein synthesis. Production of a single human ribosome requires over 200 assembly factors, 80 ribosomal proteins (r-proteins), and all three RNA polymerases and takes place in the nucleolus, nucleus, and cytoplasm of cells (Woolford and Baserga, 2013; Turowski and Tollervey, 2015; Henras et al., 2008; Kressler et al., 2010). This process is subject to complex regulation because it must be highly responsive to various cellular stimuli, such as nutrient availability (Iadevaia et al., 2014; Jastrzebski et al., 2007; Mitchell et al., 2015).

Aberrant nucleolar morphology and function have been linked to numerous human disorders, including cancer, Alzheimer's disease, and disorders of ribosome biogenesis, termed ribosomopathies (Derenzini et al., 2009, Dönmez-Altunta et al., 2005; Pich et al., 2000; Hein et al., 2013; Hariharan and Sussman, 2014; Brooks, 2017; Parlato and Kreiner, 2013; McCann and Baserga, 2013; Danilova and Gazda, 2015; Ruggero, 2012). For example, pathologists have examined nucleoli in the staging of cancers for over 200 years, with a worse prognosis correlated with increased size and number (Derenzini et al., 2017; Farley et al., 2015). Additionally, many current cancer therapeutic agents target nucleolar function because rapidly proliferating cancer cells need to increase their ribosome production (Woods et al., 2015). In some ribosomopathies, inhibited ribosome production causes a nucleolar stress response where the 5S ribonucleoprotein (RNP) complex binds MDM2 (Sloan et al., 2013; Danilova and Gazda, 2015). This leads to p53 stabilization, cell

cycle arrest, and apoptosis. Thus, nucleolar morphology is intricately linked to the creation of ribosomes and cell proliferation. Understanding the cellular mechanisms responsible for the crosstalk between nucleolar form and function could provide insights into disorders affected by changes in nucleolar morphology.

Many of the protein components involved in ribosome biogenesis were first described in the yeast *Saccharomyces cerevisiae* because of tractable biochemistry and genetics (Dixon et al., 2006; Weaver et al., 2015); however, there is growing evidence that ribosome biogenesis in human cells has acquired greater complexity in regulation (James et al., 2014; Rubbi and Milner, 2003; Zhang and Lu, 2009; Boulon et al., 2010; Vlatkovi et al., 2014; Golomb et al., 2014). Two genome-wide screens for nucleolar function have been carried out (Badertscher et al., 2015; Neumüller et al., 2013). Screens performed in *Drosophila melanogaster* and *S. cerevisiae* cells used nucleolar size as an endpoint (Neumüller et al., 2013), whereas a screen performed in HeLa cells used an assay that detects ribosome assembly and transport for the small ribosomal subunit (SSU) (Badertscher et al., 2015). However, a complete genome-wide screen for large ribosomal subunit (LSU) assembly and transport has yet to be carried out (Wild et al., 2010). Additionally, a report of an assay for nucleolar morphology in HeLa cells calculated specific parameters of abnormal-looking nucleoli, termed the iNo, but the screen was restricted to ribosomal proteins (Nicolas et al., 2016). Because human nucleolar function screens have been limited to the aneuploid HeLa cell line, and no screen has examined both SSU and LSU biogenesis genome-wide, there remain many open questions regarding the complex mechanisms that coordinate nucleolar morphology and function in human cells.

To enhance our understanding of the mechanisms regulating ribosome biogenesis in human cells, we embarked on an unbiased, genome-wide small interfering (siRNA) screening campaign using a readout of nucleolar number. Previously, we determined that defective ribosome biogenesis resulting from siRNA depletion of ribosome biogenesis factors (UTP4 and NOL11) correlates with changes in nucleolar number in human cells (Freed et al., 2012). We therefore exploited this relationship between nucleolar number and function in a genome-wide screen. The screen, conducted in the "near-normal" human MCF10A breast epithelial cell line (Soule et al., 1990), identified 139 proteins whose depletion altered the number of nucleoli per nucleus from 2–3 to only 1, uncovering 139 candidate regulators of human ribosome biogenesis. The identified proteins have a wide range of known functions and likely regulate nucleolar processes from both inside and outside of the nucleolus. To delve deeper into the specific ways in which these hits influence the production of ribosomes, we examined the effects of depleting 20 high-confidence hits on transcription of rDNA, pre-rRNA processing, and overall cellular translation. The vast majority of hits tested (90%) alter ribosome biogenesis in one or more of these assays, validating this screening approach to identify regulators of ribosome biogenesis. The results from this screen reveal how multiple cellular pathways converge in the regulation of human ribosome biogenesis and pave the way for knowledge of how ribosome biogenesis is affected in human disease.

RESULTS

A Genome-wide siRNA Screen Identifies 139 Hits as Regulators of Nucleolar Number

To identify regulators of nucleolar number in human cells, we screened 18,107 siRNAs using the GE Healthcare Dharmacon siGENOME library (Figure 1A; Table S1). MCF10A breast epithelial cells were reverse-transfected in each well of a 384-well plate with a pool of 4 siRNAs targeting the same gene of interest. Nucleoli were detected by staining with an anti-fibrillarin (FBL) antibody (Reimer et al., 1987), nuclei were detected by Hoechst, and the number of nucleoli per nucleus was quantified using a CellProfiler (Carpenter et al., 2006) pipeline (Figures 1B and S1). For each sample well, we calculated a percent effect for the change from 2–3 nucleoli per nucleus to only 1, termed the one-nucleolus phenotype. The percent effect is defined as the percentage of cells harboring 1 nucleolus normalized to the negative and positive control data from the same plate (i.e., a mean of 16 siGFP negative control wells was set as 0% effect, and the mean of 16 UTP4-positive control siRNA replicates was set as 100% effect). To monitor screen performance, coefficient of variation (CV), signal-to-background window (S/B), and Z prime (Z′) statistical parameters were calculated for each screening plate using the mean and SD of control samples. Dataset statistics indicate an average 6.8% CV and an average S/B of 4.7 (range, 3.1–8.9). The average Z′ for the screen was 0.54 (range, 0.3–0.71) (Figure 1C). Overall, these statistics demonstrate both the low variability and the high robustness of the screen.

This siRNA campaign revealed 191 screen hits that cause the one-nucleolus phenotype using a highly stringent cutoff of 3 SDs from the mean percent effect of the entire screening population (percent effect greater than 122%). This corresponds to an ~1% hit rate (Figure 1; Table S1). In an effort to eliminate any false positives, the 191 screen hits were filtered to exclude any toxic siRNAs that conferred a viability of less than 10% of the siGFP controls (Figures 1A and 1D). Any hits not expressed in breast cells (fragments per kilobase million [FPKM] = 0 in the Illumina Body Map; Petryszak et al., 2016) were also removed from the dataset, leaving 139 siRNAs that gave the one-nucleolus phenotype (Figure 1A; Table S2).

The presence of nucleolar hits validates the screening approach because it has been established that depletion of nucleolar proteins disrupts nucleolar architecture (Freed et al., 2012; Olson, 2004; Raska et al., 1990; Turner et al., 2012). Of the 139 high-confidence hits, 38 were characterized as nucleolar in 1 or more of 3 databases: the Human Protein Atlas (http://www.proteinatlas.org; Thul et al., 2017), the T cell nucleolar proteome (Jarboui et al., 2011), and the Nucleolar Proteomics Database (NOPdb) (Ahmad et al., 2009; Figure 1E).

Comparison with Existing Screens

Comparison of the hit list with hit lists of existing genome-wide screens for ribosome biogenesis factors emphasizes the ability of our screening approach to discover regulators of ribosome biogenesis. Compared with previously published genome-wide studies, we found that the screen overlap ranged from 8.5%–12.9% after correcting for interspecies conservation (Figure 1F; Table S3). Although this overlap may appear low, the differences in species and tissue type as well as the differences in screen readouts, cutoff stringency, and

lack of screen saturation may contribute. Notably, this overlap was also consistent with the overlap of the previous screens with each other (Figure 1F; Table S3).

Analysis of the Screen Hits

To identify the functional categories associated with the one-nucleolus phenotype, we explored existing algorithms that group proteins based on their gene ontology (GO) functions and high-confidence protein-protein interactions (Figure 2). GO analysis (database release date 12/28/2016) of the 139 hits shows significant ($p < 0.05$) enrichment of 42 biological processes, including translation initiation, ribosome biogenesis, rRNA processing, rRNA metabolic process, RNA catabolic process, ribonucleoprotein complex biogenesis, translation, and RNA processing (Figure 2A; Gene Ontology Consortium, 2015). Search tool for recurring instances of neighboring genes (STRING) grouping of the 139 hits shows only one major high-confidence interaction network (interaction score > 0.7), with most of the interacting partners having known functions in ribosome biogenesis and some proteins known to have roles in RNA polymerase II (Pol II) transcription (Figure 2B; Szklarczyk et al., 2015). Because our hits are enriched for proteins required for ribosome biogenesis and related cellular processes, these analyses validate the screen and highlight its ability to identify regulators of ribosome biogenesis.

Current literature supports roles for 3 of the 38 nucleolar proteins in RNAPI transcription and 5 of the 38 nucleolar proteins in ribosome biogenesis. An additional 11 of the 38 nucleolar hits are ribosomal proteins (Figure 2C). For the other 19, literature searching reveals that they are undercharacterized with regard to their specific function in ribosome biogenesis. This screen was therefore successful in identifying known regulators of ribosome biogenesis.

Validation by siRNA Deconvolution

A subset (43) of the 139 hits were chosen for validation by deconvolution of the pool of 4 siRNAs (Figure 1A; Weiss et al., 2007; Mohr et al., 2014). These hits were selected because they were undercharacterized with respect to ribosome biogenesis in the literature and/or had been implicated in human disease. Of the 43 hits, 14 are nucleolar proteins listed in existing databases and 29 are not (Ahmad et al., 2009; Jarboui et al., 2011; Thul et al., 2017). In deconvolution experiments, each of the 4 siRNAs comprising the pool used in the primary screen were tested individually. When 2 of the 4 siRNAs recapitulated the one-nucleolus phenotype by having a percent effect greater than or equal to 50%, the hit was considered validated. Of the 43 tested hits, 40 were validated using this approach, resulting in a 93% validation rate (Figure 1A; Table S4). We went on to test half of the resulting 40 hits for a functional role in making ribosomes in three secondary assays.

Rationale for Focusing on 20 Hits for Functional Assays

From the high-confidence hit list, 20 hits were chosen for an in-depth analysis of their functional roles in ribosome biogenesis (Table 1). These hits were chosen because of their originality compared with similar screens (only IQSEC3, KAT5, SUPT5H, and NMT2 were hits in previous screens; Table S3; Badertscher et al., 2015; Neumüller et al., 2013; Tafforeau et al., 2013; Wild et al., 2010) and their varying known roles in human

development and disease. The protein hits represent a panoply of diverse cellular processes, including the chromatin state of the cells and transcription (SUPT5H, KAT5, ZNF76, HIST1H2BO, and TERF2), cell division and structural organization (ANLN, NUMA1, and IQSEC3), embryonic development (LIN28A and NODAL), gene expression (NTN3 and THAP1), and cancer (CRK, PRL, and GRB2).

Of the 20 hits chosen, 10 are known to be nucleolar (Ahmad et al., 2009; Jarboui et al., 2011; Thul et al., 2017). Although KAT5 is not annotated as nucleolar in any of these databases, published literature supports nucleolar localization (Halkidou et al., 2004). Additionally, LIN28A has been characterized as nucleolar, nuclear, and cytoplasmic in different cell types and at different developmental stages but was not annotated as nucleolar in any of the databases used here (Kim et al., 2014; Chen and Carmichael, 2009; Heo et al., 2008; Balzer and Moss, 2007; Piskounova et al., 2011; Vogt et al., 2012).

7 of 20 Hits Are Required for Transcription of rDNA

Transcription of rDNA plays a key role in nucleolar architecture (Freed et al., 2012; Grob et al., 2014; Hamdane et al., 2014; Derenzini et al., 1998). Therefore, we investigated the effect of depletion of the 20 high-confidence screen hits on RNAPI transcription. RNAPI transcription was monitored using a dual-luciferase reporter assay that has previously been shown to be an accurate measure of rDNA transcription (Freed et al., 2012; Ghoshal et al., 2004). The ratios of firefly to *Renilla* luciferase were normalized to a control non-targeting siRNA (siNT). siRNAs targeting NOL11 were used as a positive control (Freed et al., 2012). Our results show that 7 of the 20 hits are required for transcription of the rDNA by RNAPI (Figure 3B). Notably, a decrease in rDNA transcription upon SUPT5H depletion was expected because the yeast ortholog Spt5p has previously been shown to interact with RNAPI and to associate with the rDNA (Schneider et al., 2006; Anderson et al., 2011; Leporé and Lafontaine, 2011). Additionally, although some studies have shown that both KAT5 and its yeast ortholog Esa1 function to downregulate rDNA transcription (Koiwai et al., 2011; Clarke et al., 2006; Chang et al., 2012), our work provides evidence for the alternative hypothesis that KAT5 increases rDNA transcription (Halkidou et al., 2004). Finally, a recent paper used different assays and experimental conditions to describe NUMA1 as an enhancer of rDNA transcription, contrary to the lack of effect on transcription reported here (Jayaraman et al., 2017).

16 of 20 Hits Are Required for Processing of the Pre-rRNA

To find out whether depletion of the 20 hits affects pre-rRNA processing, we used northern blot analysis to detect and quantify the pre-rRNAs (Figure 3). After depletion of each hit, the pre-rRNA intermediates were observed via northern blotting with 6 different oligonucleotide probes (labeled 5′ External Transcribed Spacer [5′ETS], P1, P2, 5′ITS1, P3, and P4), each detecting different pre-rRNAs (Figures 3A, 3C, and 3D and S2). The designation 1° indicates both the 47S and 45S pre-rRNA processing intermediates. Equal amounts of total RNA were loaded on each northern blot, and a probe for the 7SL RNA was used as a loading control. Ratio analysis of multiple precursors (RAMP) (Wang et al., 2014) profiles were compiled for every processing intermediate observed by probes P1, P2, P3, and P4, allowing us to obtain a snapshot of processing defects in cells depleted of each protein hit (Figure S3).

Of the 20 tested hits, 16 showed significant processing defects by the RAMP analysis (Figure S3). These defects also largely correlate with the ratio of the intermediates relative to the 7SL (Figure S4). Additionally, 3 of the 4 hits without processing defects by RAMP had significantly decreased levels of almost all intermediates relative to the 7SL loading control (Figure S4). With 3 biological replicates for each hit for the P1, P2, P3, and P4 probes, this quantitative RAMP analysis revealed the presence of 3 distinct patterns of pre-rRNA processing deficiencies (Figure 3E).

Pattern A was the most common pattern observed, characterized by defects in processing in the 5′ETS (Figure 3E). Pattern A is revealed by an increase in the 30S pre-rRNA and a concomitant decrease in its processing product, the 21S pre-rRNA. Hits included in this pathway are NODAL, LIN28A, NTN3, RBM43, NUMA1, THAP1, and IQSEC3 (see lanes 6, 7, 11, 12, 17, 21, and 23 in Figure 3C). Interestingly, this pattern has been previously seen upon depletion of a subset of r-proteins required for 5′ETS and ITS1 processing, termed initiation ribosomal proteins of the small subunit (i-RPSs) (O'Donohue et al., 2010), connecting the function of these hits to mammalian SSU biogenesis.

Pattern B involved a dramatic decrease of all intermediates relative to their precursors (Figure 3E). Protein hits in this category include ANLN, CRK, TERF2, HIST1H2BO, and PRL (see lanes 4, 9, 13, 15, and 20 in Figures 3C and 3D). Interestingly, we find that this pre-rRNA processing defect is not directly correlated with effects on rDNA transcription because, among these proteins, only HIST1H2BO and PRL depletion causes a transcription defect (Figure 3B).

Pattern C includes only one analyzed hit, ARMC2, but nevertheless shows a strikingly different defect of pre-rRNA processing (Figure 3E and lane 19 of Figure 3D). In this pattern, the 32S pre-rRNA required for making the 5.8S and 28S rRNAs accumulates, whereas the 12S pre-rRNA decreases, relative to this 32S precursor. Notably, this coincides with a decrease in the 21S pre-rRNA required to make the 18S rRNA, possibly indicating a feedback mechanism at that step of the processing pathway.

Three additional hits also had minor but significant, processing defects that did not fit into any of the above patterns: ZNF76, KAT5, and FBXW8.

Interestingly, none of the 20 tested hits showed an increase in the levels of the $30S^{+1}$ pre-rRNA, also known as the 34S pre-rRNA (Figure 3A and 5′ETS probe, data not shown). This stands in contrast to UTP4, which is the positive control for the siRNA screen and whose depletion had previously been shown to result in $30S^{+1}$ accumulation (Freed et al., 2012). In their study of SSU r-proteins, O'Donohue et al. (2010) also found very few changes in this transcript upon SSU r-protein depletion, leading them to postulate that the early cleavage step at site A' is uncoupled from the other steps in 18S formation. Additionally, none of the 20 tested hits showed significant accumulation of the 18SE pre-rRNA levels relative to the primary transcript (Figure S2C).

14 of 20 Hits Are Proteins Required for Global Cellular Translation

Defects in pre-rRNA transcription and/or processing are likely to lead to a reduction in protein synthesis. To measure this, we employed a puromycin incorporation assay (Schmidt et al., 2009). Pulses of low doses of puromycin followed by western blotting using an anti-puromycin antibody gave a robust readout of the overall levels of protein synthesis in cells depleted of each protein hit (Figure 4). Of the 20 hits examined using this assay, depletion of 14 resulted in reduced levels of global protein synthesis. As expected, most hits whose depletion did not affect ribosome biogenesis (SAMD15 and NMT2; Figure 3) also did not affect global protein synthesis.

Ultimately, we have shown that knockdown of 18 of 20 tested screen hits results in defective rDNA transcription, pre-rRNA processing, and/or global protein synthesis (Table 2). For the 2 hits that did not give a phenotype in one of these assays (SAMD15 and NMT2) and 4 hits that did give a phenotype (THAP1, KAT5, CRK, and GRB2), we performed additional qPCR experiments to demonstrate that the target mRNAs are, in fact, knocked down in MCF10A cells (Figure S5).

DISCUSSION

We have identified 139 protein regulators of nucleolar number in human cells in an unbiased genome-wide screen using a stringent cutoff (Figure 1; Table S2). Of the 20 representative validated hits we chose for functional analysis, 7 are required for pre-rRNA transcription, 16 for pre-rRNA processing, 6 for both, and 14 to maintain normal levels of protein synthesis (Table 2). Thus, our screen was highly successful in identifying a wide range of proteins that are functionally implicated in making ribosomes in the cell nucleolus. Although this information does demonstrate functional roles for 18 of 20 hits, not all steps in ribosome biogenesis were tested in our assays, including nuclear export of the ribosomal subunits. This work integrates the varied cellular functions of the 20 screen hits with the nucleolar functions of rDNA transcription, pre-rRNA processing, and global protein synthesis. Most proteins identified by this screen (69.1%) are not conserved from humans to yeast, highlighting the additional complexities of human ribosome biogenesis. The 139 screen hits include both nucleolar (27.3%) and non-nucleolar (72.7%) proteins, revealing a critical contribution to the regulation and modulation of ribosome biogenesis by proteins outside of the nucleolus in human cells.

The use of MCF10A breast epithelial cells revealed several hits, such as LIN28A, that could not have been identified by screening in other cell lines. MCF10A cells are unique in that they unexpectedly express stem cell markers, including OCT4 and SOX2 (Qu et al., 2015). Similarly, LIN28A is expressed only during embryonic development and not in many human cell lines (Piskounova et al., 2011), and, thus, its function in ribosome biogenesis has not been studied in detail. LIN28A localizes to the nucleolus during early mouse development, and lack of LIN28A arrests murine development at the 2- to 4-cell stage transition (Vogt et al., 2012). Based on its ability to bind RNA, LIN28A has been postulated to play a role in pre-rRNA processing (Daley and Sung, 2014). Additionally, it has been shown to bind and enhance the translation of several ribosomal proteins (uS17, uS15, uS11, and uS4) (Peng et al., 2011) whose depletion causes a similar pre-rRNA processing defect in HeLa cells

(O'Donohue et al., 2010) as that of the LIN28A depletion described here (Figures 3 and S3). This work therefore shows that a role for LIN28A in human ribosome biogenesis has been identified, and we have shown that LIN28A depletion does, in fact, alter pre-rRNA processing by causing an accumulation of the 30S pre-rRNA (Figures 3 and S3).

PRL is another interesting hit that was identified because of the use of MCF10A cells. We have shown here that PRL knockdown in MCF10A cells results in decreased rDNA transcription (Figure 3B). This unexpected role contributes to a body of work describing an extra-pituitary role for PRL, whose overexpression is associated with increased risk of multiple cancers (reviewed in Bernard et al., 2015; Marano and Ben-Jonathan, 2014; Sethi et al., 2012). Current therapeutic agents for breast cancer, such as the dopamine agonist bromocriptine, act at the pituitary level and so would not be effective at targeting endogenous PRL (Sethi et al., 2012). This extrapituitary role for PRL in rDNA transcription could provide insight into why current treatments targeting a secreted PRL have been unsuccessful.

Although the screen was effective in identifying a plethora of factors required for human ribosome biogenesis, the precise mechanisms regulating the formation of the one-nucleolus phenotype remain unknown. Many of the proteins we identified in this screen have known roles in cytoskeletal organization and cell division, and those studied functionally (ANLN, NUMA1, and IQSEC3) were required for pre-rRNA transcription or processing (Figure 3). Interestingly, this connects to work by the Brangwynne laboratory that postulates that cells require a scaffolding network within the nucleus to maintain nucleolar position (Feric and Brangwynne, 2013). Thus, it is possible that disruption of this scaffolding network through depletion of these cytoskeleton-related protein hits causes the nucleoli to merge into one because of gravitational sedimentation forces. Additionally, in mouse embryonic stem cells lacking upstream binding factor (UBF), it has been shown that FBL relocalizes away from the rDNA to form a nucleolar precursor body (NPB) that would be similar in appearance to the one-nucleolus phenotype (Hamdane et al., 2014, 2017). However, because many of the hits we obtained do not affect rDNA transcription (Figure 3B), it would be unlikely that the one-nucleolus phenotype is solely a measure of NPB formation. Further studies are needed to identify the precise cellular mechanism(s) regulating the formation of the one-nucleolus phenotype.

Interestingly, we have found only SSU r-proteins as hits in our screen, except for RPLP2, implying that nucleolar number may be more influenced by SSU factors than LSU factors. Indeed, SSU processing defects (pattern A; Figure 3) were the most common defects observed in our analysis of 20 screen hits. This directly contrasts with a recent siRNA screen performed only on ribosomal proteins that found that nucleolar morphology (measured by an iNo score) is more affected by depletion of LSU r-proteins than by SSU r-proteins (Nicolas et al., 2016). Such differences may be attributed to differences in screen readout and cell line used. Additionally, the iNo screen readout may not accurately reflect nucleolar function because it has been shown that depletion of both SSU and LSU r-proteins causes clear pre-rRNA processing defects (Tafforeau et al., 2013; O'Donohue et al., 2010). Notably, our screen may be enriching for SSU biogenesis factors because the positive control for this screen, UTP4, plays a role in SSU biogenesis but not LSU biogenesis.

Ribosome biogenesis is a complex and essential process that must be performed accurately and often. Therefore, human cells must be able to effectively coordinate ribosome biogenesis with a wide range of cellular cues. This screen highlights how ribosome biogenesis is enmeshed in such diverse cellular processes. Further exploration of the crosstalk between ribosome production and diverse non-nucleolar processes is essential to understanding the link between the nucleolus and human disease. This rich resource developed from our screening campaign not only increases our understanding of nucleolar regulation in human cells but could also lead to additional and better therapeutic agents for a wide range of diseases.

EXPERIMENTAL PROCEDURES

Cell Lines

MCF10A cells (ATCC, CRL-10317) were grown in DMEM/nutrient mixture F-12 (DMEM-F12, Gibco, 1130-032) supplemented with 5% horse serum (Gibco, 16050), 20 ng/mL epidermal growth factor (EGF; Sigma, E4127), 0.5 μg/mL hydrocortisone (Sigma, H0135), 100 ng/mL cholera toxin (Sigma, C8052), and 10 μg/mL insulin (Sigma, I1882) at 37°C in a humidified incubator with 5% CO_2.

siRNA Screen

In 384-well plates, MCF10A cells (3,000 cells per well) were reverse-transfected with GE Healthcare Dharmacon siGENOME library SMARTpool siRNAs (20 nM final siRNA concentration per well) using Lipofectamine RNAimax. In addition to 320 library siRNAs, each screening plate contained 16 negative control wells (GFP siRNA) and 16 positive control wells (UTP4 siRNA). After 72 hr, cells were fixed with 1% paraformaldehyde in PBS for 20 min, permeabilized with 0.5% Triton X-100 for 5 min, and blocked in 10% fetal bovine serum (FBS) in PBS for 1 hr at room temperature before immunofluorescence staining with anti-fibrillarin antibodies (72B9; Reimer et al., 1987; 1:2,000 dilution) for 2 hr at room temperature and secondary Alexa Fluor 647-conjugated goat anti-mouse immunoglobulin G (IgG) (heavy + light chain [H+L]) for 1 hr at room temperature. Hoechst 33342 (1:4,000, 1 hr at room temperature) was used to detect nuclei. After washing twice with PBS, three images per well for each of the 58 library plates were acquired using the InCell 2200 imaging system (GE Healthcare). See Supplemental Experimental Procedures for image analysis and hit selection. The complete list of screen hits can be found in Table S1.

Deconvolution of siRNA Pools

siRNA pool deconvolution was used to validate 43 hits from the genome-wide siRNA screen. MCF10A cells (3,000 cells per well) were transfected as above with the individual siRNAs corresponding to the selected hits (siGENOME, Dharmacon) in 384-well plates. After 72 hr, the cells were fixed and imaged, and the percent effect of each individual siRNA was calculated as in the genome-wide siRNA screen. A hit was considered validated when at least two of the four siRNAs met a minimum threshold of 50% effect.

RNAi

All siRNAs were purchased from Dharmacon (siGENOME). siNT (catalog no. D-001810-10-20) was also purchased from Dharmacon.

Luciferase Assays

Luciferase assays were performed as in Freed et al. (2012). See Supplemental Experimental Procedures for modifications and statistical analyses.

Northern Blotting

Northern blotting was performed as described previously (Pestov et al., 2008). See Supplemental Experimental Procedures for details, probe sequences, and statistical analyses.

Puromycin Incorporation Assay

To assess global protein synthesis, a puromycin incorporation assay was performed as in Schmidt et al. (2009). See Supplemental Experimental Procedures for modifications.

qPCR Assay

qPCR analysis was performed on selected hits using SYBR Green reagent. Because of low SAMD15 expression (cycle threshold [C_T] values > 35), we utilized the SsoAdvanced PreAMP Supermix kit from Bio-Rad (catalog no. 172-5160) to achieve appropriate C_T values for quantitation of that sample and appropriate controls. See Supplemental Experimental Procedures for cycle parameters, primer sequences, and additional details.

Supplementary Material

Refer to Web version on PubMed Central for supplementary material.

Acknowledgments

References

Ahmad Y, Boisvert FM, Gregor P, Cobley A, Lamond AI. NOPdb: Nucleolar Proteome Database–2008 update. Nucleic Acids Res. 2009; 37:D181–D184. [PubMed: 18984612]

Anderson SJ, Sikes ML, Zhang Y, French SL, Salgia S, Beyer AL, Nomura M, Schneider DA. The transcription elongation factor Spt5 influences transcription by RNA polymerase I positively and negatively. J Biol Chem. 2011; 286:18816–18824. [PubMed: 21467039]

Badertscher L, Wild T, Montellese C, Alexander LT, Bammert L, Sarazova M, Stebler M, Csucs G, Mayer TU, Zamboni N, et al. Genome-wide RNAi Screening Identifies Protein Modules Required for 40S Subunit Synthesis in Human Cells. Cell Rep. 2015; 13:2879–2891. [PubMed: 26711351]

Balzer E, Moss EG. Localization of the developmental timing regulator Lin28 to mRNP complexes, P-bodies and stress granules. RNA Biol. 2007; 4:16–25. [PubMed: 17617744]

Bernard V, Young J, Chanson P, Binart N. New insights in prolactin: pathological implications. Nat Rev Endocrinol. 2015; 11:265–275. [PubMed: 25781857]

Boulon S, Westman BJ, Hutten S, Boisvert FM, Lamond AI. The nucleolus under stress. Mol Cell. 2010; 40:216–227. [PubMed: 20965417]

Brooks WH. A review of autoimmune disease hypotheses with introduction of the "nucleolus" hypothesis. Clin Rev Allergy Immunol. 2017; 52:333–350. [PubMed: 27324247]

Carpenter AE, Jones TR, Lamprecht MR, Clarke C, Kang IH, Friman O, Guertin DA, Chang JH, Lindquist RA, Moffat J, et al. CellProfiler: image analysis software for identifying and quantifying cell phenotypes. Genome Biol. 2006; 7:R100. [PubMed: 17076895]

Chang CS, Clarke A, Pillus L. Suppression analysis of esa1 mutants in Saccharomyces cerevisiae links NAB3 to transcriptional silencing and nucleolar functions. G3. 2012; 2:1223–1232. [PubMed: 23050233]

Chen LL, Carmichael GG. Altered nuclear retention of mRNAs containing inverted repeats in human embryonic stem cells: functional role of a nuclear noncoding RNA. Mol Cell. 2009; 35:467–478. [PubMed: 19716791]

Clarke AS, Samal E, Pillus L. Distinct roles for the essential MYST family HAT Esa1p in transcriptional silencing. Mol Biol Cell. 2006; 17:1744–1757. [PubMed: 16436512]

Daley JM, Sung P. 53BP1, BRCA1, and the choice between recombination and end joining at DNA double-strand breaks. Mol Cell Biol. 2014; 34:1380–1388. [PubMed: 24469398]

Danilova N, Gazda HT. Ribosomopathies: how a common root can cause a tree of pathologies. Dis Model Mech. 2015; 8:1013–1026. [PubMed: 26398160]

Derenzini M, Trerè D, Pession A, Montanaro L, Sirri V, Ochs RL. Nucleolar function and size in cancer cells. Am J Pathol. 1998; 152:1291–1297. [PubMed: 9588897]

Derenzini M, Montanaro L, Treré D. What the nucleolus says to a tumour pathologist. Histopathology. 2009; 54:753–762. [PubMed: 19178588]

Derenzini M, Montanaro L, Trerè D. Ribosome biogenesis and cancer. Acta Histochem. 2017; 119:190–197. [PubMed: 28168996]

Dixon J, Jones NC, Sandell LL, Jayasinghe SM, Crane J, Rey JP, Dixon MJ, Trainor PA. Tcof1/Treacle is required for neural crest cell formation and proliferation deficiencies that cause craniofacial abnormalities. Proc Natl Acad Sci USA. 2006; 103:13403–13408. [PubMed: 16938878]

Dönmez-Altunta H, Akalin H, Karaman Y, Demirta H, Imamo lu N, Özkul Y. Evaluation of the nucleolar organizer regions in Alzheimer's disease. Gerontology. 2005; 51:297–301. [PubMed: 16110230]

Farley KI, Surovtseva Y, Merkel J, Baserga SJ. Determinants of mammalian nucleolar architecture. Chromosoma. 2015; 124:323–331. [PubMed: 25670395]

Feric M, Brangwynne CP. A nuclear F-actin scaffold stabilizes ribonucleoprotein droplets against gravity in large cells. Nat Cell Biol. 2013; 15:1253–1259. [PubMed: 23995731]

Freed EF, Prieto JL, McCann KL, McStay B, Baserga SJ. NOL11, implicated in the pathogenesis of North American Indian childhood cirrhosis, is required for pre-rRNA transcription and processing. PLoS Genet. 2012; 8:e1002892. [PubMed: 22916032]

Gene Ontology Consortium. Gene Ontology Consortium: going forward. Nucleic Acids Res. 2015; 43:D1049–D1056. [PubMed: 25428369]

Ghoshal K, Majumder S, Datta J, Motiwala T, Bai S, Sharma SM, Frankel W, Jacob ST. Role of human ribosomal RNA (rRNA) promoter methylation and of methyl-CpG-binding protein MBD2 in the suppression of rRNA gene expression. J Biol Chem. 2004; 279:6783–6793. [PubMed: 14610093]

Golomb L, Volarevic S, Oren M. p53 and ribosome biogenesis stress: the essentials. FEBS Lett. 2014; 588:2571–2579. [PubMed: 24747423]

Grob A, Colleran C, McStay B. Construction of synthetic nucleoli in human cells reveals how a major functional nuclear domain is formed and propagated through cell division. Genes Dev. 2014; 28:220–230. [PubMed: 24449107]

Halkidou K, Logan IR, Cook S, Neal DE, Robson CN. Putative involvement of the histone acetyltransferase Tip60 in ribosomal gene transcription. Nucleic Acids Res. 2004; 32:1654–1665. [PubMed: 15016909]

Hamdane N, Stefanovsky VY, Tremblay MG, Németh A, Paquet E, Lessard F, Sanij E, Hannan R, Moss T. Conditional inactivation of Upstream Binding Factor reveals its epigenetic functions and the existence of a somatic nucleolar precursor body. PLoS Genet. 2014; 10:e1004505. [PubMed: 25121932]

Hamdane N, Tremblay MG, Dillinger S, Stefanovsky VY, Nemeth A, Moss T. Disruption of the UBF gene induces aberrant somatic nucleolar bodies and disrupts embryo nucleolar precursor bodies. Gene. 2017; 612:5–11. [PubMed: 27614293]

Hariharan N, Sussman MA. Stressing on the nucleolus in cardiovascular disease. Biochim Biophys Acta. 2014; 1842:798–801. [PubMed: 24514103]

Hein N, Hannan KM, George AJ, Sanij E, Hannan RD. The nucleolus: an emerging target for cancer therapy. Trends Mol Med. 2013; 19:643–654. [PubMed: 23953479]

Henras AK, Soudet J, Gérus M, Lebaron S, Caizergues-Ferrer M, Mougin A, Henry Y. The post-transcriptional steps of eukaryotic ribosome biogenesis. Cell Mol Life Sci. 2008; 65:2334–2359. [PubMed: 18408888]

Heo I, Joo C, Cho J, Ha M, Han J, Kim VN. Lin28 mediates the terminal uridylation of let-7 precursor MicroRNA. Mol Cell. 2008; 32:276–284. [PubMed: 18951094]

Iadevaia V, Liu R, Proud CG. mTORC1 signaling controls multiple steps in ribosome biogenesis. Semin Cell Dev Biol. 2014; 36:113–120. [PubMed: 25148809]

James A, Wang Y, Raje H, Rosby R, DiMario P. Nucleolar stress with and without p53. Nucleus. 2014; 5:402–426. [PubMed: 25482194]

Jarboui MA, Wynne K, Elia G, Hall WW, Gautier VW. Proteomic profiling of the human T-cell nucleolus. Mol Immunol. 2011; 49:441–452. [PubMed: 22014684]

Jastrzebski K, Hannan KM, Tchoubrieva EB, Hannan RD, Pearson RB. Coordinate regulation of ribosome biogenesis and function by the ribosomal protein S6 kinase, a key mediator of mTOR function. Growth Factors. 2007; 25:209–226. [PubMed: 18092230]

Jayaraman S, Chittiboyina S, Bai Y, Abad PC, Vidi PA, Stauffacher CV, Lelièvre SA. The nuclear mitotic apparatus protein NuMA controls rDNA transcription and mediates the nucleolar stress response in a p53-independent manner. Nucleic Acids Res. 2017; 45:11725–11742. [PubMed: 28981686]

Jones TR, Kang IH, Wheeler DB, Lindquist RA, Papallo A, Sabatini DM, Golland P, Carpenter AE. CellProfiler Analyst: data exploration and analysis software for complex image-based screens. BMC Bioinformatics. 2008; 9:482. [PubMed: 19014601]

Kim SK, Lee H, Han K, Kim SC, Choi Y, Park SW, Bak G, Lee Y, Choi JK, Kim TK, et al. SET7/9 methylation of the pluripotency factor LIN28A is a nucleolar localization mechanism that blocks let-7 biogenesis in human ESCs. Cell Stem Cell. 2014; 15:735–749. [PubMed: 25479749]

Koiwai K, Noma S, Takahashi Y, Hayano T, Maezawa S, Kouda K, Matsumoto T, Suzuki M, Furuichi M, Koiwai O. TdIF2 is a nucleolar protein that promotes rRNA gene promoter activity. Genes Cells. 2011; 16:748–764. [PubMed: 21668587]

Kressler D, Hurt E, Bassler J. Driving ribosome assembly. Biochim Biophys Acta. 2010; 1803:673–683. [PubMed: 19879902]

Leporé N, Lafontaine DLJ. A functional interface at the rDNA connects rRNA synthesis, pre-rRNA processing and nucleolar surveillance in budding yeast. PLoS ONE. 2011; 6:e24962. [PubMed: 21949810]

Marano RJ, Ben-Jonathan N. Minireview: Extrapituitary prolactin: an update on the distribution, regulation, and functions. Mol Endocrinol. 2014; 28:622–633. [PubMed: 24694306]

McCann KL, Baserga SJ. Genetics. Mysterious ribosomopathies. Science. 2013; 341:849–850. [PubMed: 23970686]

Mitchell NC, Tchoubrieva EB, Chahal A, Woods S, Lee A, Lin JI, Parsons L, Jastrzebski K, Poortinga G, Hannan KM, et al. S6 kinase is essential for MYC-dependent rDNA transcription in Drosophila. Cell Signal. 2015; 27:2045–2053. [PubMed: 26215099]

Mohr SE, Smith JA, Shamu CE, Neumüller RA, Perrimon N. RNAi screening comes of age: improved techniques and complementary approaches. Nat Rev Mol Cell Biol. 2014; 15:591–600. [PubMed: 25145850]

Neumüller RA, Gross T, Samsonova AA, Vinayagam A, Buckner M, Founk K, Hu Y, Sharifpoor S, Rosebrock AP, Andrews B, et al. Conserved regulators of nucleolar size revealed by global phenotypic analyses. Sci Signal. 2013; 6:ra70. [PubMed: 23962978]

Nicolas E, Parisot P, Pinto-Monteiro C, de Walque R, De Vleeschouwer C, Lafontaine DL. Involvement of human ribosomal proteins in nucleolar structure and p53-dependent nucleolar stress. Nat Commun. 2016; 7:11390. [PubMed: 27265389]

O'Donohue MF, Choesmel V, Faubladier M, Fichant G, Gleizes PE. Functional dichotomy of ribosomal proteins during the synthesis of mammalian 40S ribosomal subunits. J Cell Biol. 2010; 190:853–866. [PubMed: 20819938]

Olson MO. Sensing cellular stress: another new function for the nucleolus? Sci STKE. 2004; 2004:pe10. [PubMed: 15026578]

Parlato R, Kreiner G. Nucleolar activity in neurodegenerative diseases: a missing piece of the puzzle? J Mol Med (Berl). 2013; 91:541–547. [PubMed: 23179684]

Peng S, Chen LL, Lei XX, Yang L, Lin H, Carmichael GG, Huang Y. Genome-wide studies reveal that Lin28 enhances the translation of genes important for growth and survival of human embryonic stem cells. Stem Cells. 2011; 29:496–504. [PubMed: 21425412]

Pestov DG, Lapik YR, Lau LF. Assays for ribosomal RNA processing and ribosome assembly. Curr Protoc Cell Biol. 2008 Chapter 22 Unit 22.11.

Petryszak R, Keays M, Tang YA, Fonseca NA, Barrera E, Burdett T, Füllgrabe A, Fuentes AMP, Jupp S, Koskinen S, et al. Expression Atlas update–an integrated database of gene and protein expression in humans, animals and plants. Nucleic Acids Res. 2016; 44(D1):D746–D752. [PubMed: 26481351]

Pich A, Chiusa L, Margaria E. Prognostic relevance of AgNORs in tumor pathology. Micron. 2000; 31:133–141. [PubMed: 10588059]

Piskounova E, Polytarchou C, Thornton JE, LaPierre RJ, Pothoulakis C, Hagan JP, Iliopoulos D, Gregory RI. Lin28A and Lin28B inhibit let-7 microRNA biogenesis by distinct mechanisms. Cell. 2011; 147:1066–1079. [PubMed: 22118463]

Qu Y, Han B, Yu Y, Yao W, Bose S, Karlan BY, Giuliano AE, Cui X. Evaluation of MCF10A as a Reliable Model for Normal Human Mammary Epithelial Cells. PLoS ONE. 2015; 10:e0131285. [PubMed: 26147507]

Raska I, Ochs RL, Andrade LE, Chan EK, Burlingame R, Peebles C, Gruol D, Tan EM. Association between the nucleolus and the coiled body. J Struct Biol. 1990; 104:120–127. [PubMed: 2088441]

Reimer G, Pollard KM, Penning CA, Ochs RL, Lischwe MA, Busch H, Tan EM. Monoclonal autoantibody from a (New Zealand black × New Zealand white)F1 mouse and some human scleroderma sera target an Mr 34,000 nucleolar protein of the U3 RNP particle. Arthritis Rheum. 1987; 30:793–800. [PubMed: 2441711]

Rubbi CP, Milner J. Disruption of the nucleolus mediates stabilization of p53 in response to DNA damage and other stresses. EMBO J. 2003; 22:6068–6077. [PubMed: 14609953]

Ruggero D. Revisiting the nucleolus: from marker to dynamic integrator of cancer signaling. Sci Signal. 2012; 5:pe38. [PubMed: 22969157]

Schmidt EK, Clavarino G, Ceppi M, Pierre P. SUnSET, a nonradioactive method to monitor protein synthesis. Nat Methods. 2009; 6:275–277. [PubMed: 19305406]

Schneider DA, French SL, Osheim YN, Bailey AO, Vu L, Dodd J, Yates JR, Beyer AL, Nomura M. RNA polymerase II elongation factors Spt4p and Spt5p play roles in transcription elongation by RNA polymerase I and rRNA processing. Proc Natl Acad Sci USA. 2006; 103:12707–12712. [PubMed: 16908835]

Schneider CA, Rasband WS, Eliceiri KW. NIH Image to ImageJ: 25 years of image analysis. Nat Methods. 2012; 9:671–675. [PubMed: 22930834]

Sethi BK, Chanukya GV, Nagesh VS. Prolactin and cancer: Has the orphan finally found a home? Indian J Endocrinol Metab. 2012; 16(Suppl 2):S195–S198. [PubMed: 23565377]

Sloan KE, Bohnsack MT, Watkins NJ. The 5S RNP couples p53 homeostasis to ribosome biogenesis and nucleolar stress. Cell Rep. 2013; 5:237–247. [PubMed: 24120868]

Soule HD, Maloney TM, Wolman SR, Peterson WD Jr, Brenz R, McGrath CM, Russo J, Pauley RJ, Jones RF, Brooks SC. Isolation and characterization of a spontaneously immortalized human breast epithelial cell line, MCF-10. Cancer Res. 1990; 50:6075–6086. [PubMed: 1975513]

Szklarczyk D, Franceschini A, Wyder S, Forslund K, Heller D, Huerta-Cepas J, Simonovic M, Roth A, Santos A, Tsafou KP, et al. STRING v10: protein-protein interaction networks, integrated over the tree of life. Nucleic Acids Res. 2015; 43:D447–D452. [PubMed: 25352553]

Tafforeau L, Zorbas C, Langhendries JL, Mullineux ST, Stamatopoulou V, Mullier R, Wacheul L, Lafontaine DL. The complexity of human ribosome biogenesis revealed by systematic nucleolar screening of Pre-rRNA processing factors. Mol Cell. 2013; 51:539–551. [PubMed: 23973377]

Thul PJ, Åkesson L, Wiking M, Mahdessian D, Geladaki A, Ait Blal H, Alm T, Asplund A, Björk L, Breckels LM, et al. A subcellular map of the human proteome. Science. 2017; 356:eaal3321. [PubMed: 28495876]

Turner AJ, Knox AA, Watkins NJ. Nucleolar disruption leads to the spatial separation of key 18S rRNA processing factors. RNA Biol. 2012; 9:175–186. [PubMed: 22418842]

Turowski TW, Tollervey D. Cotranscriptional events in eukaryotic ribosome synthesis. Wiley Interdiscip. Rev RNA. 2015; 6:129–139. [PubMed: 25176256]

Vlatkovi N, Boyd MT, Rubbi CP. Nucleolar control of p53: a cellular Achilles' heel and a target for cancer therapy. Cell Mol Life Sci. 2014; 71:771–791. [PubMed: 23685903]

Vogt EJ, Meglicki M, Hartung KI, Borsuk E, Behr R. Importance of the pluripotency factor LIN28 in the mammalian nucleolus during early embryonic development. Development. 2012; 139:4514–4523. [PubMed: 23172912]

Wang M, Anikin L, Pestov DG. Two orthogonal cleavages separate subunit RNAs in mouse ribosome biogenesis. Nucleic Acids Res. 2014; 42:11180–11191. [PubMed: 25190460]

Weaver KN, Watt KE, Hufnagel RB, Navajas Acedo J, Linscott LL, Sund KL, Bender PL, König R, Lourenco CM, Hehr U, et al. Acrofacial dysostosis, Cincinnati type, a mandibulofacial dysostosis syndrome with limb anomalies, is caused by POLR1A dysfunction. Am J Hum Genet. 2015; 96:765–774. [PubMed: 25913037]

Weiss WA, Taylor SS, Shokat KM. Recognizing and exploiting differences between RNAi and small-molecule inhibitors. Nat Chem Biol. 2007; 3:739–744. [PubMed: 18007642]

Wild T, Horvath P, Wyler E, Widmann B, Badertscher L, Zemp I, Kozak K, Csucs G, Lund E, Kutay U. A protein inventory of human ribosome biogenesis reveals an essential function of exportin 5 in 60S subunit export. PLoS Biol. 2010; 8:e1000522. [PubMed: 21048991]

Woods SJ, Hannan KM, Pearson RB, Hannan RD. The nucleolus as a fundamental regulator of the p53 response and a new target for cancer therapy. Biochim Biophys Acta. 2015; 1849:821–829. [PubMed: 25464032]

Woolford JL Jr, Baserga SJ. Ribosome biogenesis in the yeast Saccharomyces cerevisiae. Genetics. 2013; 195:643–681. [PubMed: 24190922]

Zhang Y, Lu H. Signaling to p53: ribosomal proteins find their way. Cancer Cell. 2009; 16:369–377. [PubMed: 19878869]

Highlights

- Genome-wide siRNA screen for human proteins that regulate nucleolar number

- Biochemical analyses of the 139 hits found roles for 18/20 in ribosome biogenesis

- The results reveal an orchestrated gene network that co-regulates ribosome assembly
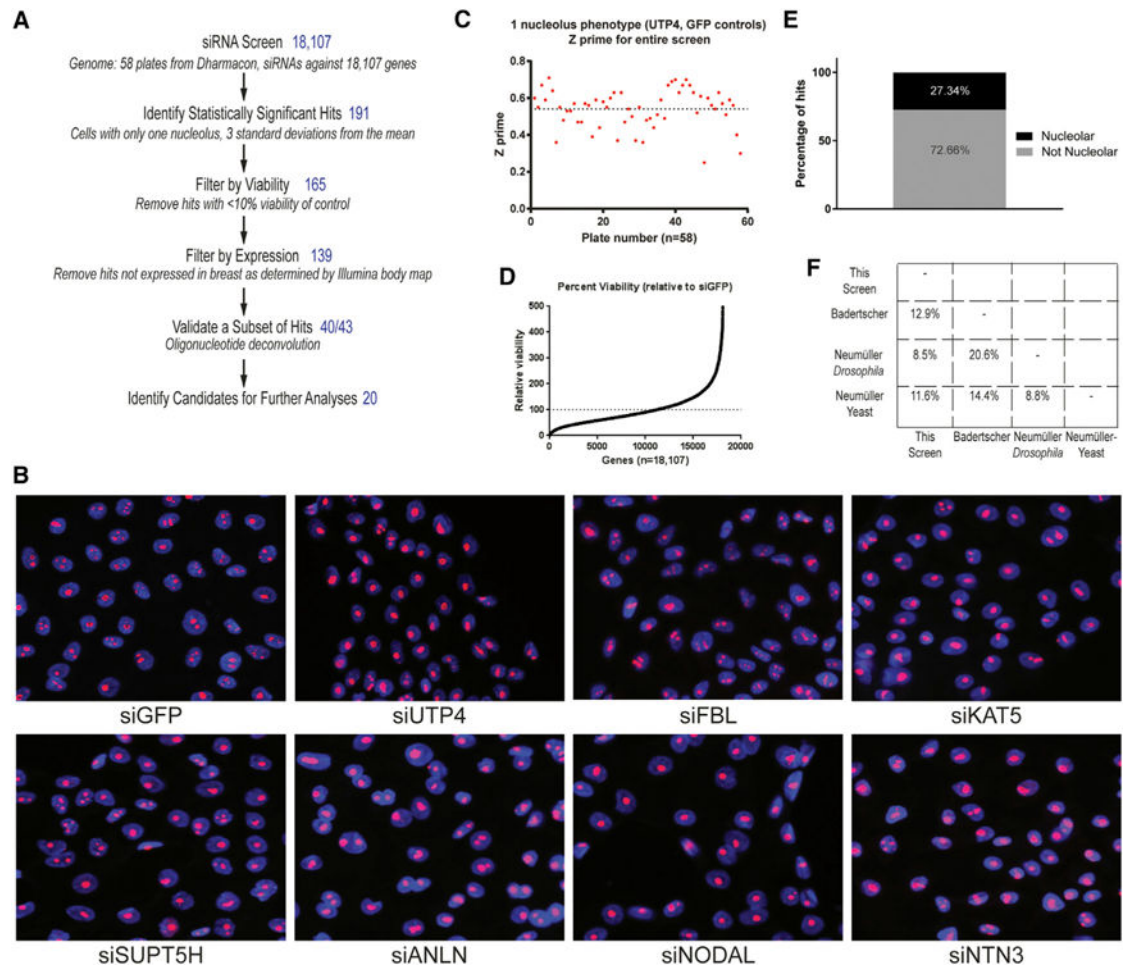
Figure 1. Genome-wide siRNA Screen Reveals 139 High-Confidence Regulators of Nucleolar Number

(A) Workflow of the screening campaign. In 384-well plates, MCF10A cells were reverse-transfected with pools of siRNAs targeting 18,107 genes (each pool consisting of 4 individual siRNAs targeting a single gene). After 72 hr, the cells were stained with antibodies to fibrillarin (α-fibrillarin, to detect nucleoli) and Hoechst (to detect nuclei). Nucleoli and nuclei were segmented, and the number of nucleoli per nucleus were counted using a pipeline developed in CellProfiler (Jones et al., 2008). Hits (191) were identified whose depletion changed the number of nucleoli from 2–3 to 1, termed the one-nucleolus phenotype. These hits were filtered by viability (> 10% relative to siGFP control) and expression (FPKM > 0 in Illumina Body Map; Petryszak et al., 2016), leaving 139 high-confidence hits. Of the high-confidence hits, 40 of 43 were validated in a secondary oligonucleotide deconvolution screen, where at least 2 of the 4 individual siRNAs gave the one-nucleolus phenotype (50% effect). Of the validated candidates, 20 were chosen for further analyses via secondary assays.

(B) Representative images from the screen showing the one-nucleolus phenotype for six screen hits. The negative and positive controls are also shown (siGFP and siUTP4, respectively). Nuclei are shown in blue (Hoechst). Nucleoli are shown in red (α-fibrillarin).

Histograms showing the frequency of the number of nucleoli per nucleus for the 20 candidates chosen for further analyses and the controls can be found in Figure S1.

(C) Z′ factors for the genome-wide siRNA screen by plate relative to the siUTP4 and siGFP controls. The dashed line shows an average Z′ of 0.54.

(D) Percent viability of each siRNA pool (n = 18,107) relative to the siGFP negative control. A dashed line is drawn at 100% viability.

(E) Percentage of hits identified as nucleolar (black) or not nucleolar (gray) in existing databases (Jarboui et al., 2011; Ahmad et al., 2009; Thul et al., 2017).

(F) Diagram showing the percent of overlap between this screen and existing genome-wide siRNA screens for ribosome biogenesis factors (Badertscher et al., 2015; Neumüller et al., 2013) when corrected for species conservation. "Badertscher" refers to the screen for SSU biogenesis performed in Badertscher et al. (2015). "Neumüller *Drosophila*" and "Neumüller Yeast" refer to the screens for nucleolar size performed in *Drosophila* and *Saccharomyces cerevisiae*, respectively, performed in Neumüller et al. (2013).
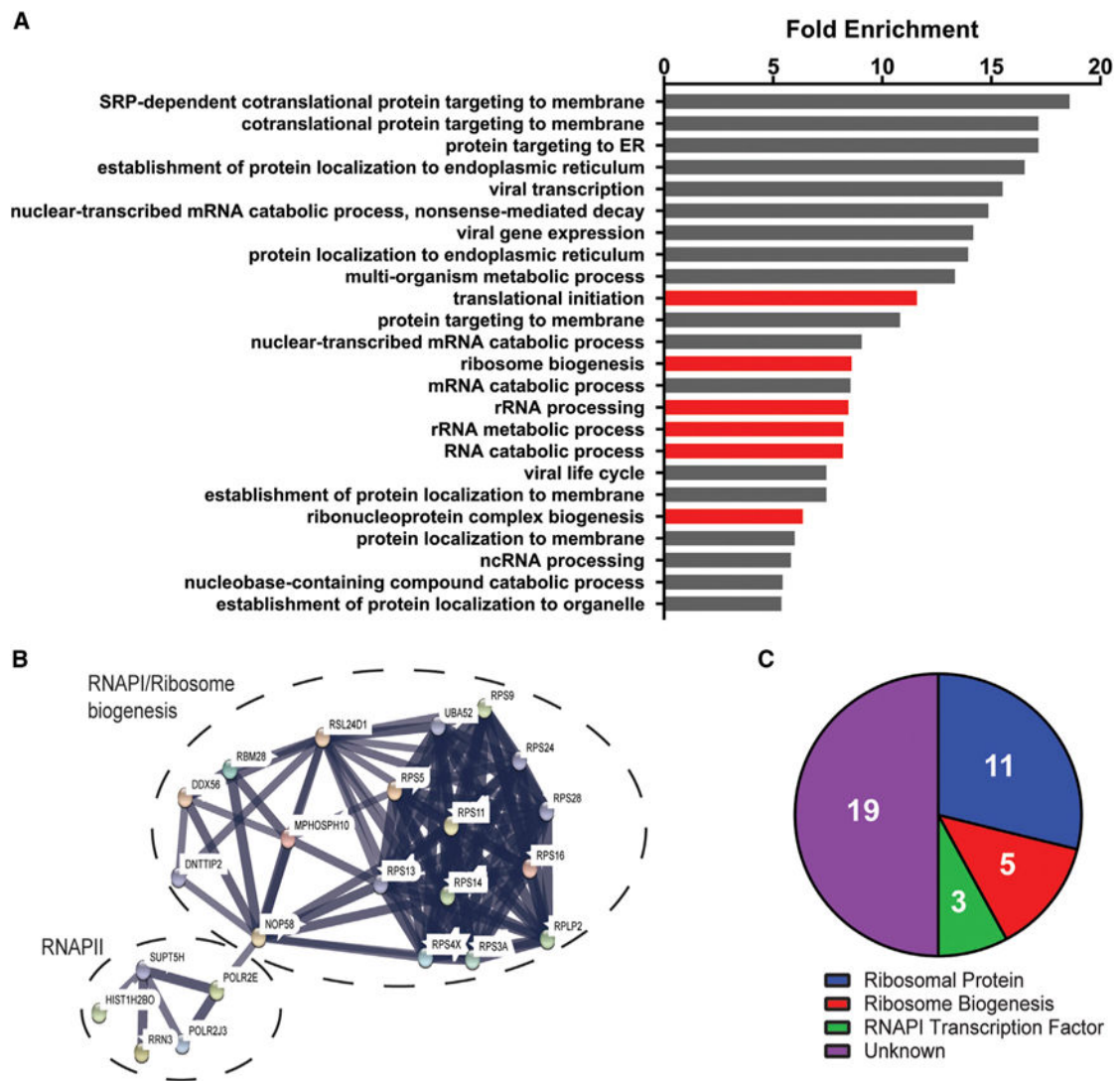
Figure 2. Functional Analysis of the 139 High-Confidence Screen Hits Shows Enrichment of Ribosome Biogenesis Factors

(A) GO analysis (Gene Ontology Consortium, 2015; p 0.05, fold enrichment 5) of the 139 screen hits reveals enrichment of 6 biological processes (red bars) related to ribosome biogenesis.

(B) STRING grouping shows one large high-confidence interaction network (interaction score > 0.7) that can be further separated into two functional units (dashed circles): RNAPI/ ribosome biogenesis factors and Pol II transcription-related factors.

(C) Pie chart showing that the 38 hits annotated as nucleolar in existing databases (Jarboui et al., 2011; Ahmad et al., 2009; Thul et al., 2017) can be separated into 4 functional categories: ribosomal proteins (blue), ribosome biogenesis factors (red), RNA polymerase I (RNAPI) transcription factors (green), and unknown function (purple).
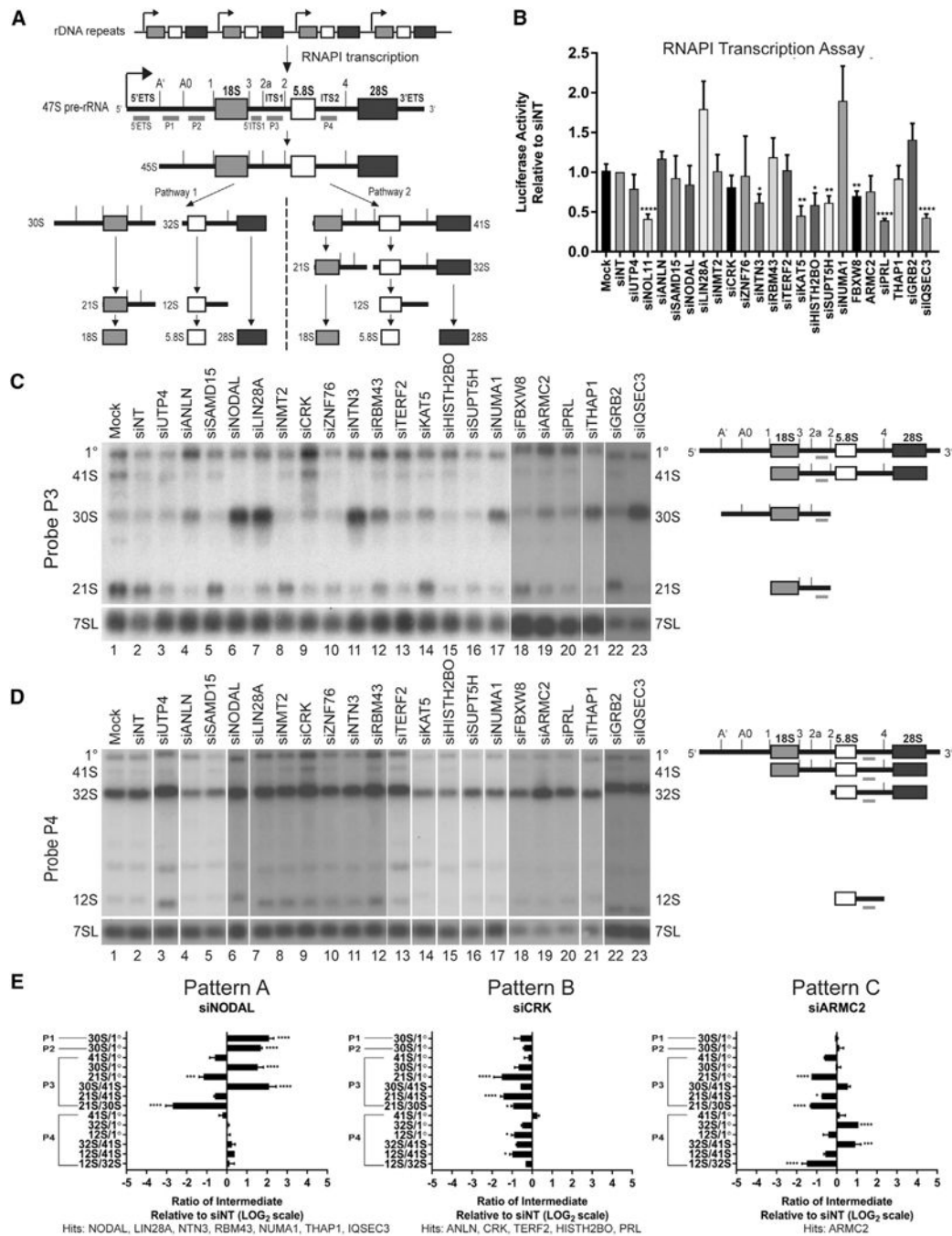
Figure 3. Functional Testing of 20 Hits for Roles in RNAPI Transcription and Pre-rRNA Processing

(A) Overview of the human pre-rRNA transcription and processing that forms the mature 18S, 5.8S, and 28S rRNAs. The repeated rDNA is transcribed by RNAPI into the 47S pre-rRNA. The 47S pre-rRNA is further processed through one of two major pathways into the mature rRNAs that are incorporated into the small (18S) and large (5.8S and 28S) ribosomal subunits. Probes for northern blots (5′ETS, P1, P2, P3, 5′ITS1, and P4) are shown in gray below the 47S pre-rRNA.

(B) Depletion of 7 of 20 hits results in decreased RNAPI transcription. MCF10A cells were transfected with the indicated siRNAs. After 48 hr, two plasmids were transfected: one containing firefly luciferase under the control of the rDNA promoter (pHrD-IRES-Luc) (Ghoshal et al., 2004) and a *Renilla* luciferase transfection control (Freed et al., 2012). Twenty-four hours later, luminescence was measured using a 20/20n luminometer (Turner Biosystems) and the Dual Luciferase Reporter Assay System (Promega). The ratio of firefly to *Renilla* luciferase activity was normalized to the siNT control. Data are shown as mean ± SEM; n = 3. Significance was calculated by Student's t test using GraphPad Prism. *p 0.05, **p 0.01, ***p 0.001, ****p 0.0001.

(C) Depletion of 16 of 20 hits results in defective pre-rRNA processing. Shown is a northern blot analysis of the 20 selected hits using a probe for the ITS1 (P3). siRNAs targeting each hit as well as mock, siNT, and siUTP4 controls were transfected into MCF10A cells. Seventy-two hours later, RNA was harvested and analyzed by northern blot (probe P3). A probe for the 7SL RNA is shown as a loading control. A diagram of the pre-rRNA processing intermediates detected by probe P3 is shown to the right. 1° indicates the 47S and 45S pre-rRNA processing intermediates.

(D) Northern blot analysis of the 20 selected hits using a probe for the ITS2 (P4) as in (C).

(E) RAMP analysis (Wang et al., 2014) reveals three major patterns of pre-rRNA processing defects among the 20 selected hits. RNAs were quantitated from the northern blots with each of the 6 probes shown in (A) using a PhosphorImager. Representative RAMP profiles for probes P1, P2, P3, and P4 are shown below each pattern, as well as a list of hits that give that pattern when siRNA-depleted. Probes used to detect each ratio are listed to the left of each RAMP profile. Data are shown as mean ± SEM, relative to siNT, on a $\log_2$ scale; n = 3. Significance was calculated by two-way ANOVA with Sidak's multiple comparisons test using GraphPad Prism. *p 0.05, ****p 0.0001. RAMP profiles of all 20 analyzed hits and controls are shown in Figure S3. 1° indicates the 47S and 45S pre-rRNA processing intermediates.
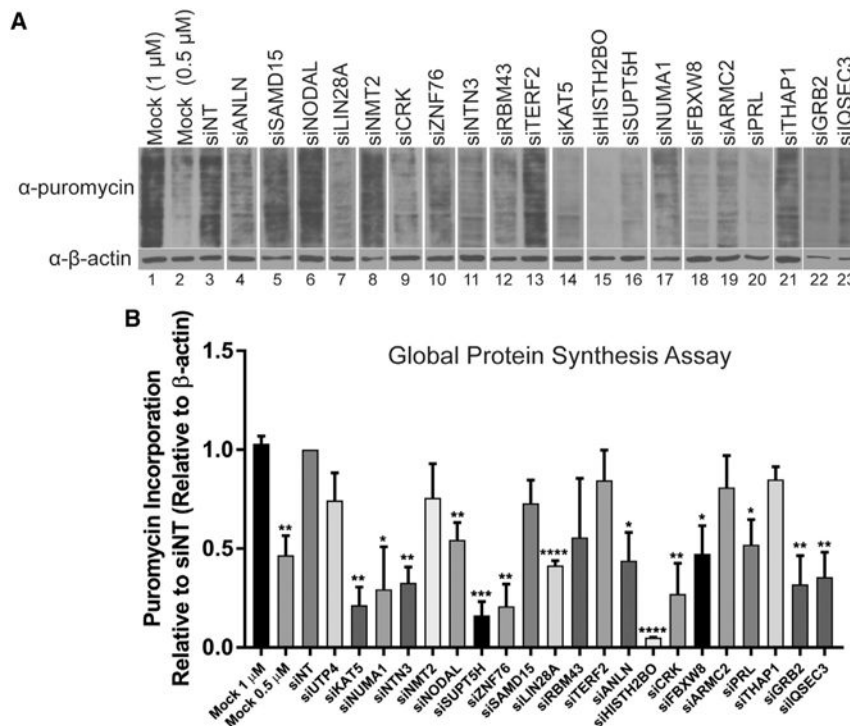
Figure 4. Global Protein Synthesis Is Reduced upon Depletion of 14 of 20 Hits of Interest
(A) MCF10A cells were transfected with the indicated siRNAs for 72 hr. Cells were then pulsed with 1 μM puromycin (or 0.5 μM for the mock half-dose control) for 1 hr at 37°C before harvesting protein and western blotting with α-puromycin antibodies. An antibody to β-actin was used as a loading control.

(B) Quantitation of the global protein synthesis assay. ImageJ (Schneider et al., 2012) was used to quantify the relative puromycin incorporation for cells depleted with the indicated siRNAs relative to siNT and the β-actin loading control. Data are shown as mean ± SEM; n = 3. Significance was calculated by Student's t test using GraphPad Prism. *p 0.05, **p 0.01, ***p 0.001, ****p 0.0001.

Table 1

High-Confidence Screen Hits Chosen for Further Analyses

Protein Name	HGNC Symbol	Nucleolar/Non-nucleolar	Description
Anillin actin binding protein	ANLN	nucleolar	actin-binding protein with a role in cytokinesis
Armadillo repeat-containing 2	ARMC2	non-nucleolar	armadillo repeat containing
CRK proto-oncogene, adaptor protein	CRK	non-nucleolar	adaptor protein involved in multiple signaling pathways, proto-oncogene
F-box and WD repeat domain containing 8	FBXW8	non-nucleolar	F-box protein, substrate recognition component ubiquitin protein ligase complex
Growth factor receptor-bound protein 2	GRB2	non-nucleolar	adaptor protein that links cell receptors to the Ras signaling pathway
Histone cluster 1 H2B family member o	HIST1H2BO	nucleolar	core component of the nucleosome
IQ motif and Sec7 domain 3	IQSEC3	non-nucleolar	guanine nucleotide exchange factor
Lysine acetyltransferase 5	KAT5	non-nucleolar	histone acetyltransferase
Lin-28 homolog A	LIN28A	non-nucleolar	N-terminal myristoyltransferase
N-myristoyltransferase 2	NMT2	non-nucleolar	N-terminal myristoyltransferase
Nodal growth differentiation factor	NODAL	non-nucleolar	essential for mesoderm formation and axial patterning
Netrin 3	NTN3 non-nucleolar	system	may function in axon guidance during nervous system development
Nuclear mitotic apparatus protein 1	NUMA1	nucleolar microtubules	pole in mitotic spindle formation, binds microtubules
Prolactin	PRL	non-nucleolar	pituitary hormone
RNA binding motif protein 43	RBM43	non-nucleolar	contains an RNA binding motif
Sterile alpha motif domain containing 15	SAMD15	nucleolar	contains a sterile alpha motif
SPT5 homolog, DSIF elongation factor subunit	SUPT5H	nucleolar	component of DRB sensitivity-inducing factor complex, role in Pol II transcriptional elongation and mRNA processing
Telomeric repeat binding factor 2	TERF2	nucleolar	binds and stabilizes telomeres
THAP domain-containing 1	THAP1	non-nucleolar	DNA-binding pro-apoptotic factor
Zinc-finger protein 76	ZNF76	nucleolar	zinc-finger domain, transcriptional regulator

DRB, 5,6-Dichloro-1-β-D-ribofuranosylbenzimidazole.

Table 2

Summary of Defects in Pre-rRNA Transcription, Processing, or Global Protein Synthesis after Depletion of the 20 Selected Hits

HGNC Symbol	Transcription	Processing	Global Protein Synthesis
ANLN	–	pattern B	Y
ARMC2	–	pattern C	–
CRK	–	pattern B	Y
FBXW8	Y	misc	Y
GRB2	–	–	Y
HIST1H2BO	Y	pattern B	Y
IQSEC3	Y	pattern A	Y
KAT5	Y	misc	Y
LIN28A	–	pattern A	Y
NMT2	–	–	–
NODAL	–	pattern A	Y
NTN3	Y	pattern A	Y
NUMA1	–	pattern A	Y
PRL	Y	pattern B	Y
RBM43	–	pattern A	–
SAMD15	–	–	–
SUPT5H	Y	–	Y
TERF2	–	pattern B	–
THAP1	–	pattern A	–
ZNF76	–	misc	Y

Yes (Y) indicates defective transcription or global protein synthesis. Pattern A/B/C indicates the RAMP processing defect patterns shown in Figures 3E and S3. misc, miscellaneous.